DOE/ER/3072-39
September 9, 1986

PROPOSAL FOR AN EXPERIMENTAL STUDY OF NONLINEAR THOMSON SCATTERING

R.C. FERNOW and H.G. KIRK
Brookhaven National Laboratory

I.J. BIGIO and N.A. KURNIT
Los Alamos National Laboratory

K.D. BONIN, K.T. McDONALD,† and D.P. RUSSELL
Princeton University

Submitted to Brookhaven National Laboratory

† Spokesperson

Summary

We propose to investigate nonlinear Thomson scattering as the first experiment in a program to study the nonlinear quantum electrodynamics of electrons and photons in an intense electromagnetic wave. A laser beam of 10-μm wavelength, 2-picosecond pulse duration, and peak intensity 10^{16} Watts/cm^2 will be brought into head-on collision with a single bunch of 40-MeV electrons at the Brookhaven Accelerator Test Facility. At such intensities it is probable that an electron absorbs several laser photons before emitting a single photon of higher energy. In addition, the transverse oscillations of an electron inside the laser beam are relativistic, which leads to a shift in the effective mass of the electron that is discernible in the spectrum of radiated photons.

In the laboratory the laser beam is backscattered into x-rays. The peak brightness of the resulting beam of x-rays will exceed that available at any existing source, although the pulse repetition rate will only be a few per second. An x-ray spectrometer based on Bragg scattering off a graphite mosaic crystal will analyze the scattered light. Data collection for the experiment should take only about one week. The observation of x-ray production via e-laser collsions will, we believe, be an essential diagnostic as to the successful synchronization of the laser and linac beams for any purpose.

1. Theoretical Context.

In the proposed experiment we wish to explore the simplest nonlinear interaction of a free electron with an intense electromagnetic wave. This work will serve as the starting point of an extended program of study of nonlinear quantum electrodynamics, as outlined in some detail in reference 1.

In the present experiment a 40-MeV electron beam is brought into head-on collision with a 10-μm-wavelength laser beam. The latter is so intense that an electron absorbs several laser photons before it emits a photon that carries away the sum of the energies of the absorbed photons. In the rest frame of the electron beam the laser photons have 20-eV energy, so the scattering process is well described as the classical limit of Compton scattering, namely Thomson scattering. The effect of multiphoton absorption may then be termed nonlinear Thomson scattering.

In classical language, the criterion for the onset of nonlinear effects is that the transverse motion of the electron induced by the laser beam be relativistic. A useful measure of this is the field-strength parameter η, defined by

$$\eta \equiv \frac{eE}{m\omega c} = \gamma_\perp \beta_\perp,$$

where $\gamma_\perp = 1/\sqrt{1-\beta_\perp{}^2}$, $\beta_\perp = v_\perp/c$, $v_\perp$ is the transverse velocity of the electron, and E and ω are the electric-field strength and the angular frequency of the laser beam. For electrons in a wave with $\eta \gtrsim 1$ the magnitude of the radiation of the oscillating quadrupole (or higher) moment is comparable to dipole radiation. Of course, the higher multipole radiation occurs at higher harmonics of the oscillation frequency, which is equivalent to the earlier description that several photons are absorbed from the wave before a higher energy photon is emitted.

In plasma physics the quantity $eE/m\omega c$ is often called $v_{\rm osc}/c$. As we are particularly interested in the regime where the value of this quantity exceeds 1, we adopt the new notation, η.

It is useful to record some numerical relations between η, the electric-field strength E, and the wave intensity I. First note that

$$I\ [\text{Watts/cm}^2] = \frac{\langle E^2 \rangle}{377\ [\text{ohms}]} \qquad \text{for } E \text{ in V/cm}.$$

Hence

$$E_{\rm r.m.s.}\ [\text{V/cm}] = 19.4\sqrt{I\ [\text{Watts/cm}^2]}.$$

Then we find

$$\eta^2 = 3.7 \times 10^{-19} I\lambda^2 \qquad \text{for } I \text{ in Watts/cm}^2 \text{ and } \lambda \text{ in } \mu\text{m}.$$

For example, with $\lambda = 10$ μm ($\hbar\omega = 0.124$ eV), as in the proposed experiment, $\eta = 1$ corresponds to intensity $I = 2.7 \times 10^{16}$ Watts/cm^2, and in turn to an electric field strength of $E = 3 \times 10^9$ V/cm.

At the focus of a diffraction-limited laser beam the intensity is related to the beam power by $I \sim P/(2\pi\lambda^2)$, so we have the approximate result

$$\eta^2 \sim 5 \times 10^{-12} P[\text{Watts}],$$

independent of the laser wavelength.

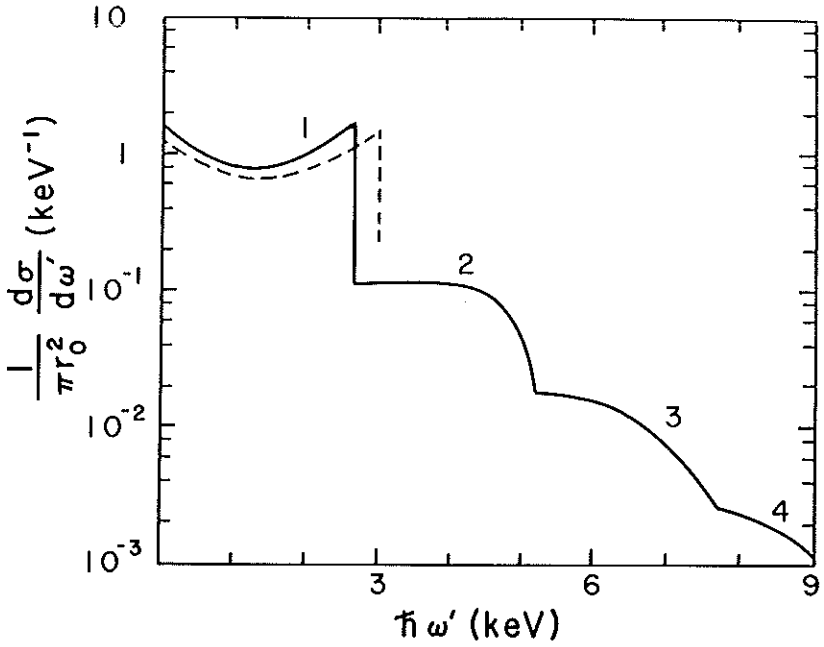

Figure 1. The differential cross section for nonlinear Thomson scattering of a 40-MeV electron beam in head-on collision with a plane electromagnetic wave of 10-μm wavelength and field-strength parameter $\eta = 0.4$, as a function of the energy $\hbar\omega'$ of the scattered photons. The contributions due to absorption of 1 through 4 wave photons are labeled. The dashed curve is the ordinary Thomson cross section. Note the shift in the end point of the one-photon energy spectrum.

A classical calculation of the radiation was first given by Schott[2] in 1912, which can be shown to be the correct limit of a quantum-mechanical calculation for nonlinear Compton scattering.[3] Figure 1 shows the results of such a calculation for

a 40-MeV electron placed in a plane wave of 10-μm wavelength and field-strength parameter $\eta = 0.4$. The Doppler shift gives dipole-radiation photons energies up to 3 keV. Higher multipole radiation leads to the shoulders at higher photon energies seen in the figure.

An important effect related to the relativistic transverse motion of the electrons is the shift in the endpoint energy of the dipole-radiation spectrum, also seen in Figure 1. This arises in the Doppler-shift calculation because the boost to the (average) rest frame of the electron must take into account the transverse energy of the electron. This behavior can be summarized by saying that an electron in an intense wave field has an effective mass

$$\overline{m} = m\sqrt{1+\eta^2}.$$

Thus the endpoint energy, $\hbar\omega'_{\max}$, of the spectrum of the n^{th}-harmonic radiation is

$$\hbar\omega'_{\max} = \frac{4nE^2\hbar\omega}{\overline{m}^2c^4 + 4nE\hbar\omega},$$

where ω is the frequency of the laser and E is the electron energy. The 'mass-shift' effect on the energy spectrum will be a useful signature that the electron beam has actually passed through an intense-field region of the laser beam.

The proposed experiment will observe the essential features of nonlinear Thomson scattering: the higher harmonic compenents of the scattered light, and the mass-shift effect on the endpoint of the dipole-radiation spectrum. There has been only one previous experimental study of this subject,[4] in which the η of the laser field was 0.01. This permitted detection of a very weak component of second-harmonic radiation, but did not allow any verification of the mass-shift effect.

2. Overview of the Experiment.

The experimental configuration is sketched in Figure 2.

The 40-MeV electron beam will be produced by the Brookhaven Lab Accelerator Test Facility (ATF), whose rather small emittance, $1.8(\pi) \times 10^{-10}$ rad-m permits the electron beam to be focused to a spot of radius 0.5 μm with a depth of focus $\beta^* = 1.6$ mm.† The laser beam is brought into head-on collision with the

† The depth of focus is the distance from the focal plane at which the spot size has grown by a factor of 2 in area. In accelerator argot, this is called the β^*, while in laser lingo it is called the confocal parameter or, sometimes, the Rayleigh range.

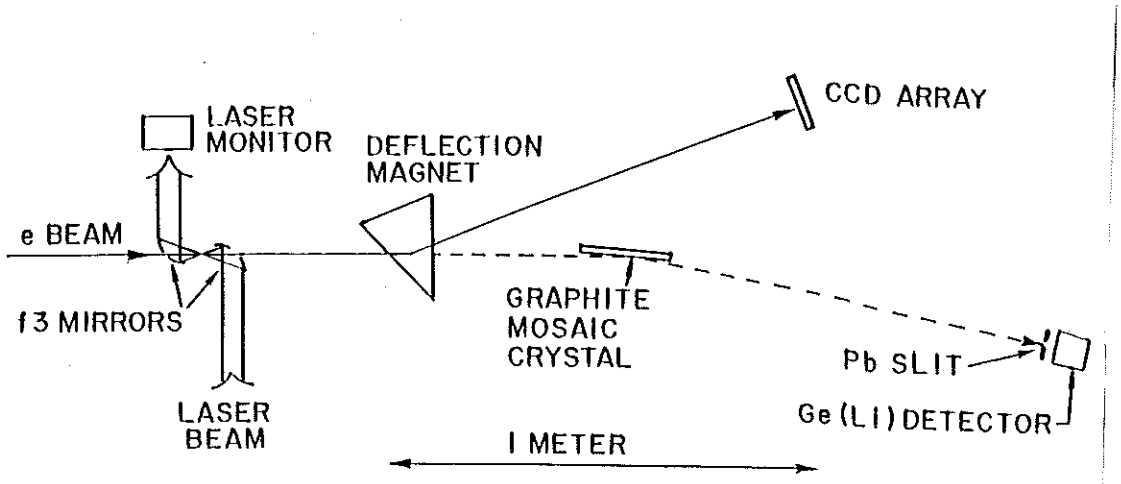

Figure 2. Layout of the proposed experiment.

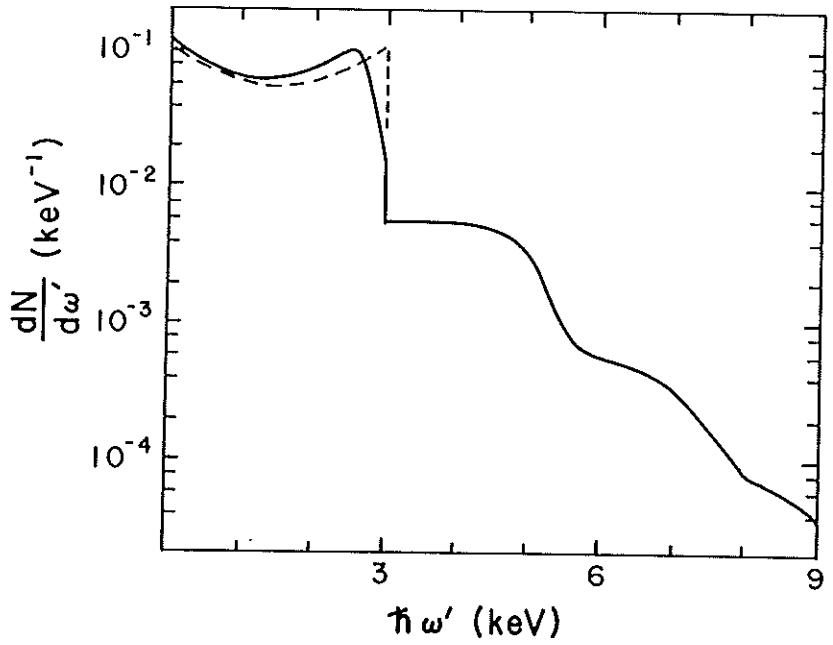

Figure 3. The scattering rate for a single 40-Mev electron in head-on collision with a laser beam of wavelength 10 μm. The laser pulse has 0.1-Joule energy and 2-ps pulse length, and is focused in an $f3$ mirror to achieve peak field-intensity parameter $\eta = 0.4$ The total scattering rate is 0.25 per electron. The dashed curve is the rate for Thomson scattering if nonlinear effects are ignored.

electrons by an off-axis parabolic mirror with $f/d = 3$. A hole of $\sim$ 1-mm diameter in the mirror lets the electron beam and the backscattered photons pass through. The unscattered laser beam will be collected in a second mirror and reflected out of the electrons' path into a beam-flux monitor. The electrons are deflected by 23° in a dipole magnet 0.5 m downstream of the collision point, and their momentum spectrum recorded by the CCD array. Photons which are backscattered to within 10 mrad of the electron-beam direction are analyzed in an x-ray spectrometer located 1 m downstream of the collision point.

For an estimate of the scattering rate we suppose both the electron bunch and the laser pulse have FWHM of 2 ps. The laser beam has total energy of 0.1 Joule. The electron and photon beams are taken to have Gaussian radial profiles. The confocal parameter for the laser beam is 200 μm when it is focused by the $f3$ mirror. The above variations of electron and photon flux over the interaction volume are then combined with the cross section to give the scattering rate.

Figure 3 summarizes the spectrum of scattered photons. The total scattering rate is 0.25 per beam electron. Thus the probability that an electron scatters twice while crossing the laser beam is 0.06. This places an important constraint on the x-ray detector, that it be able to tell a double scatter at the first harmonic from the rarer case of a single scatter at the second harmonic. The detector will not be able to resolve multiple photons in time during the 2-ps pulse, but must deflect x-rays of different energies by different angles so they can be separately counted. This is provided by a detector based on Bragg scattering off a graphite crystal.

Because the intensity of the laser beam is nonuniform near the focus the endpoint of the dipole-scattering spectrum is not sharp. Most of the scattering occurs in the high-field region, leading to the peak at 2.6 keV, while the rarer scattering in the low-field region populates the x-ray spectrum up to the unshifted endpoint of 3.0 keV. Despite this, the mass-shift effect will be clearly discernible in the data.

In the following sections we discuss briefly the electron beam, the laser system, the e-laser interaction region, the spectrometer to monitor the electron beam, the x-ray spectrometer, backgrounds, and the scenario for data collection.

3. The Electron Beam.

Some basic parameters of the proposed Accelerator Test Facility are summarized in Table 1. The original proposal called for a single accelerating section powered by a 36-MW klystron. It now appears that the available klystron will be rated to closer to 30 MW, so the nominal beam energy would be closer to 40 MeV. If

Table 1. Accelerator Test Facility Specifications

Parameter	
Photocathode gun voltage	400 kV
Photocathode gun pulse length (FWHM)	2 ps
Photocathode laser wavelength	0.532 μm
Cathode radius	20 μm
Transverse energy at cathode	$\sim$ 0.1 eV
Invariant emittance out of gun ϵ_n	1.35×10^{-8} mc-m
Cathode current density	200 A/cm^2
Electrons per bunch	$\sim 10^5$
Beam energy	40 MeV
Klystron peak power	30 MW
Klystron repetition rate	$\leq$ 180 pps
Electron energy spread $\Delta E/E$ (FWHM)	$\sim$ 0.1%
Geometric transverse emittance at experiment	1.8×10^{-10} rad-m

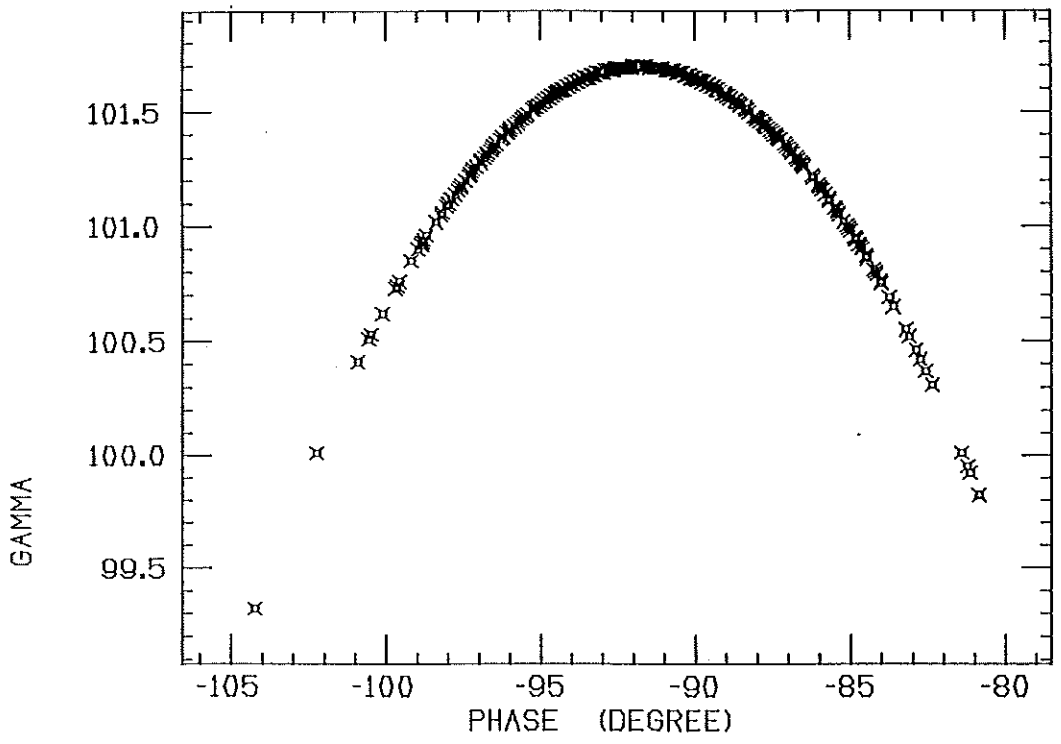

Figure 4. Electron-beam energy, $E = \gamma mc^2$, as a function of the rf phase, for 50-MeV nominal beam energy.

a second accelerator section and klystron are added, 80-MeV beams would also be available.

The very low emittance (1.8×10^{-10} m-rad) is to be achieved with a very small illumination (20-μm radius) at the photocathode of the electron gun, and with a very small transverse energy (0.1 eV) of the electrons ejected from the cesium-antimony photocathode.[5]

Figure 4 illustrates how the accelerated electron energy, $E = \gamma mc^2$, varies with the phase of the electron relative to the 2856-MHz accelerating field. At this frequency 1° of phase equals 0.97 ps in time. The stated electron-energy spread of $\Delta E/E = 0.1\%$ derives from an assumption of a 2-ps bunch length, synchronized to the rf to 1-ps accuracy, as described in section 4, and also that the electrons' paths through the gun are isochronous to the needed accuracy.

The electron beam is brought from the linac to the experiment in a beam transport which permits a final focus of 0.5-μm radius. The corresponding beam divergence is 3×10^{-4} radians, and the depth of focus is $\beta^* = 1.6$ mm. Emittance-defining collimators along the beam transport will allow cleanup of the beam and further reduction of the emittance, if desired. If a momentum-analysis section is included in the beam transport, the beam energy spread could be collimated to 0.01%, with a loss in beam intensity.

The linac structure and any collimators in the beam transport are a likely a source of x-rays, which will be the principal source of background for the experiment. This background would be greatly reduced by a bend in the beamline, as would be provided by a momentum-analysis section.

4. The Laser System.

The laser system for the present experiment is an upgraded version of that to be built at Los Alamos National Lab for the laser-grating-accelerator experiment.[6] In principle either the laser front end (1-μm wavelength) or the CO_2 amplifier (10-μm wavelength) could be improved to achieve the desired field-strength of $\eta = 0.4$. Effort devoted to obtaining higher power pulses at 10-μm wavelength will pay off in the enhanced performance of the Accelerator Test Facility as an x-ray source, and is considered in the present proposal. An alternative scheme based on upgrading the 1-μm-wavelength front end of the laser is considered in ref. 1.

A block diagram of the laser system and its interconnection with the electron linac is shown in Figure 5. Both the laser and the linac derive their timing reference signals from a highly stable reference oscillator. The laser front end is a mode-locked

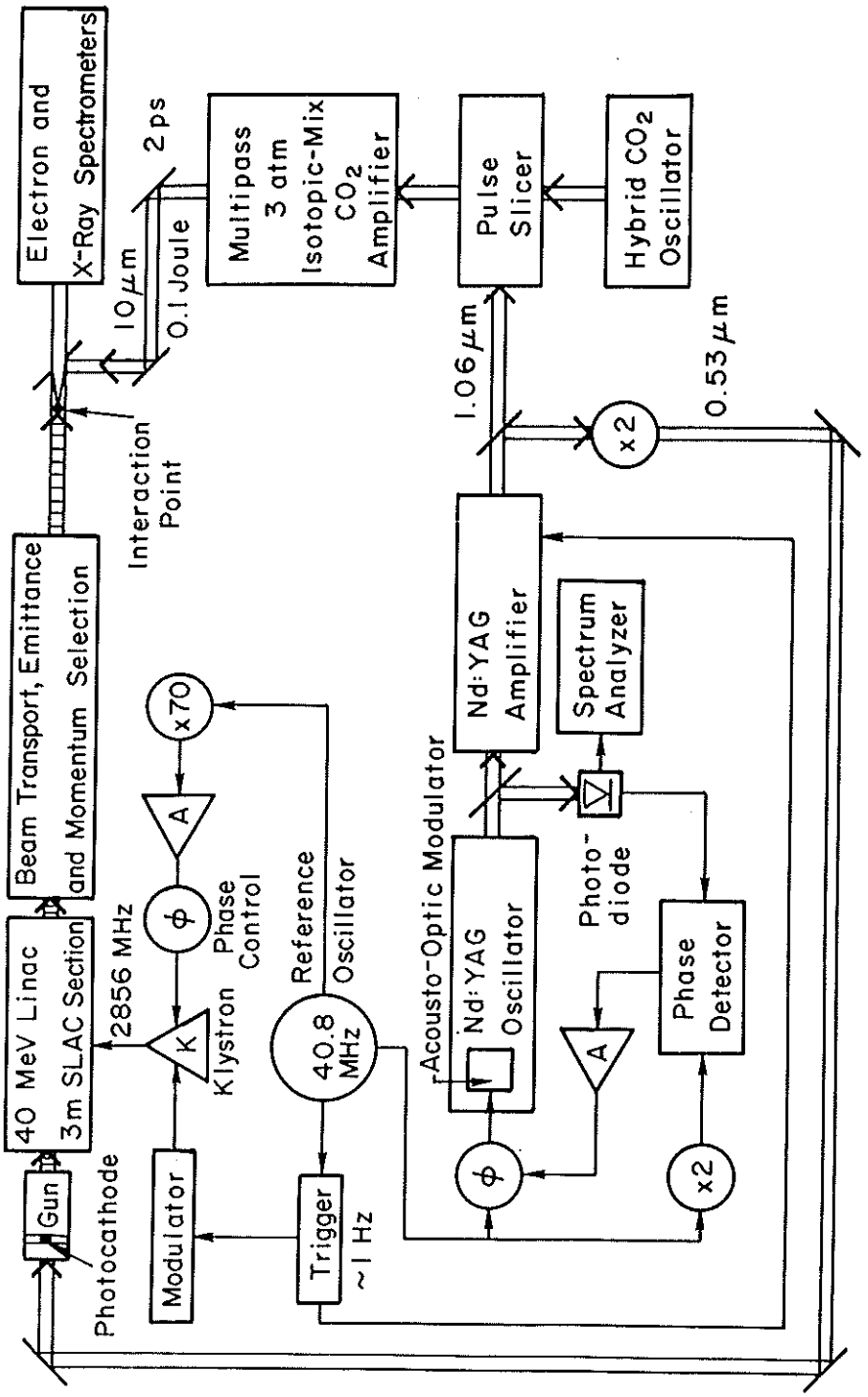

Figure 5. Block diagram of the laser system and its synchronization with the electron linac.

cw Nd:YAG oscillator which is also phase locked to the reference oscillator via a feedback loop.[7] A few pulses per second from the Nd:YAG oscillator are amplified and compressed. These serve to trim the long output pulses of the hybrid CO_2 oscillator into pulses of 2-ps duration.[8] The short CO_2 pulses are then amplified to energy greater than 0.1 Joule in a multipass gain module filled with a mix of CO_2 isotopes. If desired, an additional gain module could be added to achieve extremely high pulse energies.

5. The Interaction Region.

The laser beam is brought to a focus in a head-on collision at the final focus of the electron beam. The power level of the laser beam is 100 GW, which requires the use of reflection optics. An off-axis parabolic mirror of $f/d = 3$ focal length/aperture will focus the laser beam. The mirror radius will be 2 cm, sufficient to intercept the growth of the laser beam between the laser and the mirror. Hence the mirror will be located 12 cm from the e-laser interaction point. At this distance the electron beam radius is 36 μm r.m.s. The electron beam will pass through a 1-mm-diameter hole in the mirror, as sketched in Figure 2.

The unscattered laser beam will be collected in a second parabolic mirror, and brought to a beam-flux monitor. To aid in alignment of the mirrors with respect to the electron beam a quadrant detector will be located on the upstream face of the second mirror. The two mirrors will be mounted together on an x-y-z translation stage capable of 0.1-μm steps, such as manufactured by Klinger.

The interaction region will be maintained at a vacuum of 10^{-5}-10^{-6} torr. The drive motors for the translation stage could be located inside the vacuum chamber while maintaining a vacuum of 10^{-6} torr. The vacuum chamber will be constructed to be interchangeable with that for the laser-grating experiments at the Accelerator Test Facility.

6. The Electron Spectrometer.

After the electron beam passes the interaction point, it must be deflected to one side to allow the scattered photons to be analyzed. The magnet required for this also serves as the dispersive element in a precision electron spectrometer, sketched in Figure 2.. The dipole magnet has a field of 1400 Gauss, a field integral of 0.053 Tesla-m (for the 40-MeV beam), and deflects the electrons by 23°. The electron beam then impinges on a CCD array with 385 × 580 pixels each 25-μm square, located 1 m downstream of the deflection magnet. The spectrometer will be capable of 2-keV resolution for the 40-MeV electrons.

The spectrometer will serve as the primary electron-beam-flux monitor, measuring the beam intensity as a function of momentum.

The electron spectrometer will be in a different configuration from that used in the laser-grating experiment,[6] with the magnet now immediately after the interaction region to improve the acceptance of the x-ray spectrometer. The quadrupole triplet, which provides a line focus on the CCD array for the laser-grating experiment, will not be needed. Only about 50 columns of the CCD array will be populated with electrons in the present experiment. If the readout is restricted to these columns the readout dead-time would be reduced by a factor of 8, permitting data collection at about 10 pps.

7. The X-Ray Spectrometer.

As shown in Figure 3, laser photons that backscatter off the electron beam are Doppler-shifted to x-ray energies. During a 2-ps pulse of 10^5 electrons we expect 2.5×10^4 x-rays to be produced. To analyze these we need an x-ray spectrometer which disperses x-rays of different energies to different positions. Then a total absorption detector which counts the number of x-rays at a fixed position will determine the x-ray flux within a well-defined energy bin.

The nonlinear mass-shift effect (at the proposed laser intensity) reduces the endpoint of the x-ray spectrum by some 15% compared to weak-field Thomson scattering. (See Figure 3.) Thus bins of 1% in x-ray energy would be quite suitable to analyze the effect. This is 10–100 times broader than the bandwidth of a typical x-ray monochromator which uses a perfect crystal. However, our requirements are well matched to the capability of a spectrometer based on a flat pyrolitic graphite crystal,[9] in which there is a spread (or mosaic) of 0.8° in the orientations of the planes of the microcrystals.

The simultaneous functioning of the graphite crystal as a dispersive and focusing element is sketched in Figures 6 and 7. We are fortunate in having a very good approximation to a point source at the electron-photon interaction region. This is shown at distance L from the center of the crystal, which is oriented at the Bragg angle θ_B for x-rays of energy E. An x-ray of energy E traveling along the central ray will penetrate into the crystal until it meets a microcrystal with its crystal planes at angle θ_B to the x-ray. The x-ray then scatters by angle $2\theta_B$ with about 40% efficiency.

Now consider an x-ray also of energy E, but which makes angle $\Delta/2$ to the central ray, as shown in Figure 6. If the graphite were in the form of a single perfect

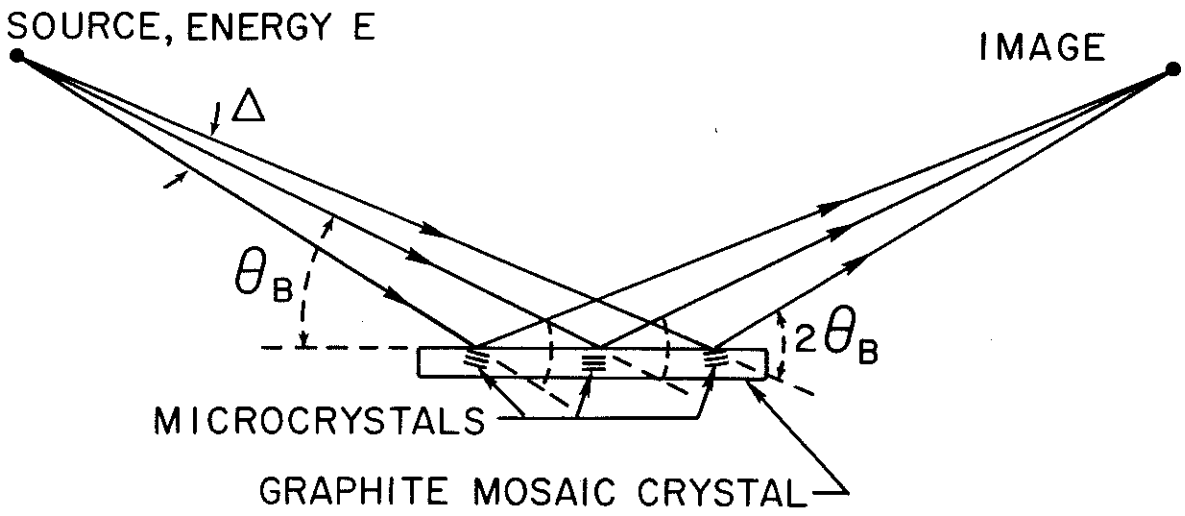

Figure 6. The scattering of monoenergetic x-rays by a graphite mosaic crystal. The scattering angle is always twice the Bragg angle θ_B. The mosaic spread, Δ, of orientations of the microcrystals results in a focusing geometry with angular acceptance Δ.

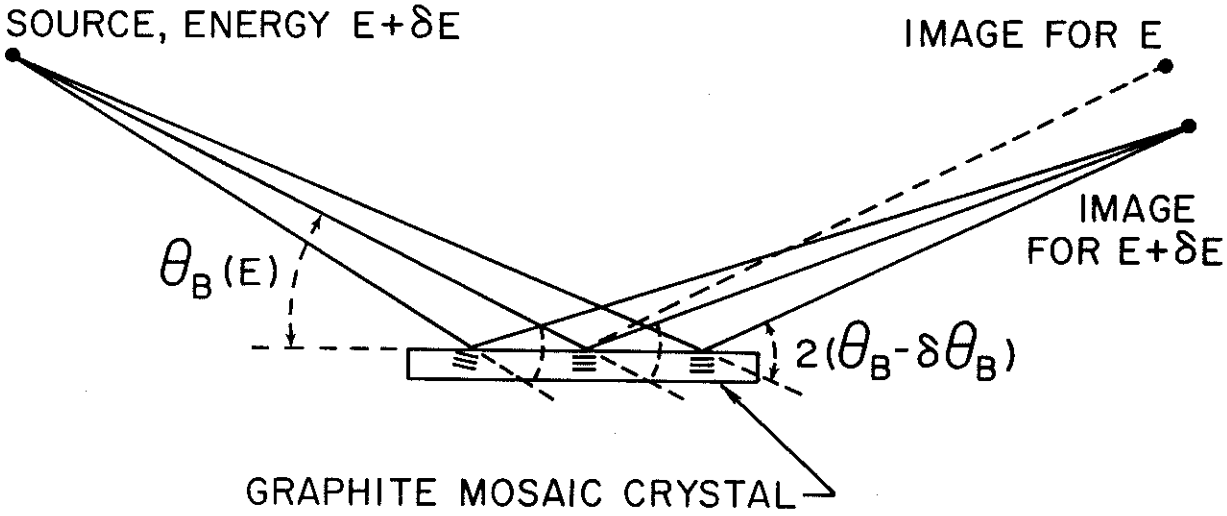

Figure 7. X-rays of energy $E + \delta E$ are focused by Bragg reflection off a graphite mosaic crystal to a different point than those of energy E.

crystal, this x-ray would not strike the crystal planes at the Bragg angle θ_B, and would not be scattered. But if Δ is less than or equal to the mosaic spread of the graphite crystal then the x-ray does scatter off some microcrystal, again with scattering angle $2\theta_B$. The paths of the two scattered x-rays cross approximately at distance L from the crystal. That is, the variable orientation of the microcrystals within the flat macroscrystal duplicates the focusing effect (in the scattering plane only) of a bent perfect crystal.

Next consider the case of x-rays with energy $E + \delta E$, as shown in Figure 7. The corresponding Bragg angle is now $\theta_B - \delta\theta_B$. Such an x-ray traveling along the central ray at angle θ_B to the crystal could not scatter off a perfect crystal. But if $\delta\theta_B < \Delta/2$, the x-ray will find some microsrystal off which it can scatter, with scattering angle $2(\theta_B - \delta\theta_B)$. Similarly, x-rays of energy $E + \delta E$ which make small angles to the central ray also scatter off some microsrystal, and are brought to a focus at distance L from the crystal. Because of the dependence of the Bragg angle on x-ray energy, the scattered x-rays disperse along a focal plane as desired.

For numerical computation it is useful to note the Bragg relation for graphite:

$$\sin\theta_B = \frac{1.85}{E[\text{keV}]}.$$

This follows from the usual form of Bragg's law,

$$\sin\theta_B = \frac{\lambda}{2d},$$

the useful conversion formula

$$\lambda[\text{Å}] = \frac{12.38}{E[\text{keV}]},$$

and the fact that the crystal plane separation in graphite is $2d = 6.71$ Å. The dispersive effect can be calculated by taking the derivative of the Bragg law:

$$\cot\theta_B\,\delta\theta_B = \frac{\delta E}{E},$$

which is well aproximated in graphite for $E \gtrsim 10$ keV by

$$\delta\theta_B = \frac{1.85}{E[\text{keV}]}\frac{\delta E}{E}.$$

For example, with $E = 3$ keV, the Bragg angle is 665 mrad, so the scattering angle is 76°. For a 1% bite $\delta E/E$ about 3 keV, the angular bite is $\delta\theta_B = 7.86$

mrad. If the distance L from the source to the crystal, and hence from crystal to the detector, is 1 m, then a slit of 7.8 mm at the face of the detector would define the 1% energy acceptance.

The angular acceptance (in the scattering plane) of the spectrometer is in prinicple limited only by the mosaic spread angle $\Delta = 0.8° = 14$ mrad. To take full advantage of this range the crystal must have length

$$l = \frac{L \cdot \Delta}{\sin\theta_B} = \frac{L \cdot \Delta \cdot E[\text{keV}]}{1.85}.$$

We wish to analyze the third harmonic scattering, for which $E \sim 9$ keV, so this requires crystal length $l \sim 7$ cm.

The flat-crystal geometry of the spectrometer does not provide any focusing transverse to the scattering plane. With source and detector equidistant from the crystal, the transverse size of the image is twice that of the intercept of the x-rays at the crystal. With a Ge(Li) detector of 50-mm diameter, the useful width of the graphite crystal is then 25 mm. Hence there will be acceptance for x-rays which make angle θ of up to 12.5 mrad with respect to the direction of the electron beam. As just noted, there cannot be full angular acceptance for angles $\theta > \Delta/2 = 7$ mrad.

There is an additional effect on the transverse size of the image on the detector. Due to the mosaic spread, Δ, of the microcrystals, the x-rays of a given energy which scatter from a given point on the graphite crystal have a spread of angles, Δ, in azimuth. The x-rays scatter at polar angle 2θ and describe an arc of length $l = L \cdot \Delta \cdot \sin\theta$ over the face of the detector. For $L = 1$ m, $\Delta = 14$ mrad, and $\theta_B = .665$ corresponding to 3 keV, we have arc length $l = 9$ mm.

In summary, the configuration of the x-ray spectrometer is simple and classic. The graphite crystal is mounted on a rotating stage located 1 m from the e-laser interaction point, along the line of the electron beam (see Figure 2). X-rays of a given energy are brought to a focus 1 m from the crystal, after scattering at twice the Bragg angle. A slit defines the width of the energy bin, and the number of x-rays in that bin is determined by measurement of the sum of their energies in a Ge(Li) solid-state detector, such as Ortec Model GLP-50/10.

Figure 8 shows the relation between x-ray energy and angle θ relative to the direction of the electron beam for the first three harmonics in nonlinear Thomson scattering. Because the electron beam will pass through regions of various laser-beam intensity, there is a range of x-ray energies produced at any fixed angle.

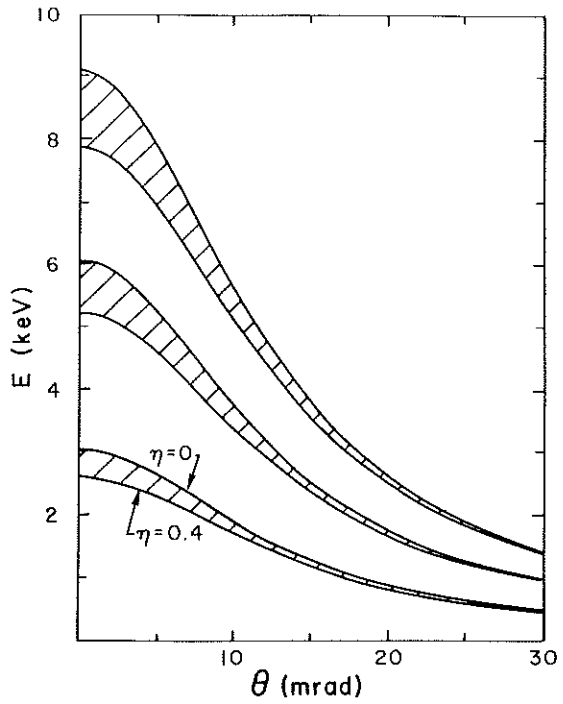

Figure 8. The relation between x-ray energy and production angle for the first three harmonics in nonlinear Thomson scattering of 40-MeV electrons and a 10-μm laser beam. The bands are due to the intensity dependence of the nonlinear effects.

The bands in Figure 8 show this range corresponding to field-strength parameter η between 0 and 0.4. The scattering rate will be much higher on the $\eta = 0.4$ edge of the bands. With a graphite crystal of mosaic spread angle $\Delta = 14$ mrad, there will be full collection efficiency out to production angle 7 mrad. The collection efficiency at larger angles will be determined experimentally by a calibration run with reduced laser intensity, so that $\eta \sim 0$ and we may utilize the well-known spectrum of x-rays from linear Thomson scattering.

8. Backgrounds.

Background x-rays could arise from synchrotron radiation in the dump magnet (or beam-momentum-selection magnets if present), from bremsstrahlung of the electron beam off residual gas in the vacuum chamber, or from bremsstrahlung off the emittance-defining collimators in the beam line. The latter effect is likely to be the most serious, but is hard to estimate quantitatively. Considerable care will be required to install the necessary shielding against this source. We now show that the other two sources may be calculated to be negligible.

Concerning synchrotron radiation, recall that the characteristic frequency ra-

diated by an electron of energy $E = \gamma mc^2$ in a magnetic field B is

$$\omega \sim \gamma^3 \omega_o = \gamma^2 \frac{eB}{mc} = 511\gamma^2 \frac{B}{B_{\rm cr}}[\text{keV}],$$

where $B_{\rm cr} = m^2c^3/e\hbar = 4.41 \times 10^{13}$ Gauss. Thus for $E = 40$ MeV and $B = 1400$ Gauss we find $\omega = 0.1$ eV, which is hardly in the x-ray range. Furthermore, the total energy radiated in one revolution is

$$\frac{\Delta E}{E} = \frac{4\pi}{3}\alpha\gamma^2 \frac{B}{B_{\rm cr}}.$$

For a 23° bend and the above parameters for E and B, we have $\Delta E = 0.02$ eV, or 0.2 radiated photon per electron. Clearly there can be no significant tail into the keV region.

Concerning scattering off residual gas, suppose we have as much as 10 m path in a vacuum of 10^{-5} torr. Assuming the residual gas to be air, the radiation length at this pressure is then 2×10^{10} m. For 10^5 electrons of 40-MeV energy traversing 10 m of this gas, the total radiated energy is about 8 keV. Hence we might expect a few x-rays per pulse. A vacuum of 10^{-6} torr would render the residual gas background completely negligible.

9. Data Collection.

Both the readout of the CCD array of the electron spectrometer, and thermal limitations of the final laser amplifier may limit the repetition rate of the experiment to less than 10 pulses per second. For the purpose of rate estimates we assume only one pulse per second.

The expected rate of x-ray production per electron is presented in Figure 3, for laser operation at design intensity. As noted in section 2, up to 10^5 electrons per pulse can be provided by the Accelerator Test Facility. With a total scattering probablility of 0.25 per electron, some 2.5×10^4 x-rays will be produced each pulse. These are largely due to first harmonic scattering, which populates the 0–3 keV region of the x-ray spectrum. In a 1% energy bin (30 ev) we then expect about 250 x-rays per pulse. Statistical accuracy of 2% would be obtained with only 10 pulses.

The graphite-mosaic-crystal spectrometer will collect x-rays only within about 10 mrad of the electron-beam direction. Refering to Figure 8, we see that we will be able to explore readily only the upper 30% of the energy range of each harmonic. That is, some 30 spectrometer settings of 1% bandwidth would constitute a data run at each harmonic.

According to Figure 3, the data rate at the third harmonic will be about 1/1000 that at the first harmonic. Good statistical accuracy could then be obtained in one hour of running, 3600 pulses. A scan of 30 spectrometer settings would take one day.

In section 7 we mentioned the need to calibrate the x-ray spectrometer on the ordinary Thomson-scattering spectrum obtained with a low-intensity laser beam. To avoid any nonlinear mass-shift effect on the spectrum to the 1% level, the laser field-intensity parameter η^2 should be less than 0.001. (Recall from section 1 that the position of the 'Compton edge' of the energy spectrum is multiplied by $\sim 1/(1+\eta^2)$ in a strong field.) As the laser-photon flux is also proportional to η^2, the scattering rate would then be 160 times smaller than that at the nominal operating condition of $\eta = 0.4$. Thus in the calibration run, which can only explore the first harmonic scattering, there will be about 2 x-rays per pulse in a 1% energy bin. Calibration data should be collected for about one hour at each spectrometer setting, for a total of one day's running. To calibrate the spectrometer at energies above 3 keV, the electron beam energy will be raised. For example, 6-keV x-rays will be studied with 56-MeV electrons, and 9-keV x-rays with 70-MeV electrons, noting that the scattered x-ray energy varies as the square of the electron-beam energy. In each case the calibration should take about one day.

Thus once the apparatus is fully working, the entire data collection could be performed in about 24 hours, with final calibration occupying several days. We feel this is consistent with the nature of a demonstration experiment, in which the greatest amount of time will be spent in perfecting the novel technologies required.

References

1. K.T. McDonald, 'Proposal for Experimental Studies of Nonlinear Quantum Electrodynamics,' DOE/ER/3072-38, Princeton University (Sept. 1986).
2. G.A. Schott, *Electromagnetic Radiation*, (Cambridge University Press, 1912).
3. For a textbook discussion, see V.B. Berestetskii *et al.*, *Quantum Electrodynamics*, (Pergamon Press, 1982), §101, p. 449.
4. T.J. Englert and E.A. Rinehart, 'Second-Harmonic Photons from the Interaction of Free Electrons with Intense Laser Radiation,' Phys. Rev. **A 28**, 1539 (1983).
5. C.K. Sinclair and R.H. Miller, 'A High Current, Short Pulse, RF Synchronized Electron Gun for the Stanford Linear Accelerator,' IEEE Trans. Nuc. Sci. **NS-28**, 2649 (1981).
6. R.B. Palmer *et al.*, 'Laser Accelerator Test Beam,' (August 27, 1985), unpublished.
7. M.J.W. Rodwell *et al.*, 'Reduction of Timing Fluctuations in a Mode-Locked Nd:YAG Laser by Electronic Feedback,' submitted to Opt. Lett.
8. P.B. Corkum, 'Amplification of Picosecond 10-μm Pulses in Multiatmosphere CO_2 Lasers,' IEEE J. QE-**21**, 216 (1985).
9. R.W. Gould *et al.*, 'Application of the Graphite Monochromator to Light-Element X-Ray Spectroscopy,' Appl. Spectr. **22**, 549 (1968); C.J. Sparks, Jr., 'Mosaic Crystals for Obtaining Larger Energy Bands and High Intensities from Synchrotron Radiation Sources,' in *Workshop on X-Ray Instrumentation for Synchrotron Radiation Research*, ed. by H. Winick and G. Brown (SSRL Report 78/04, Stanford, 1978), p. III-35.